INSTITUTE FOR NONLINEAR STUDIES

DISTRIBUTION STATEMENT A
Approved for public release;
Distribution Unlimited

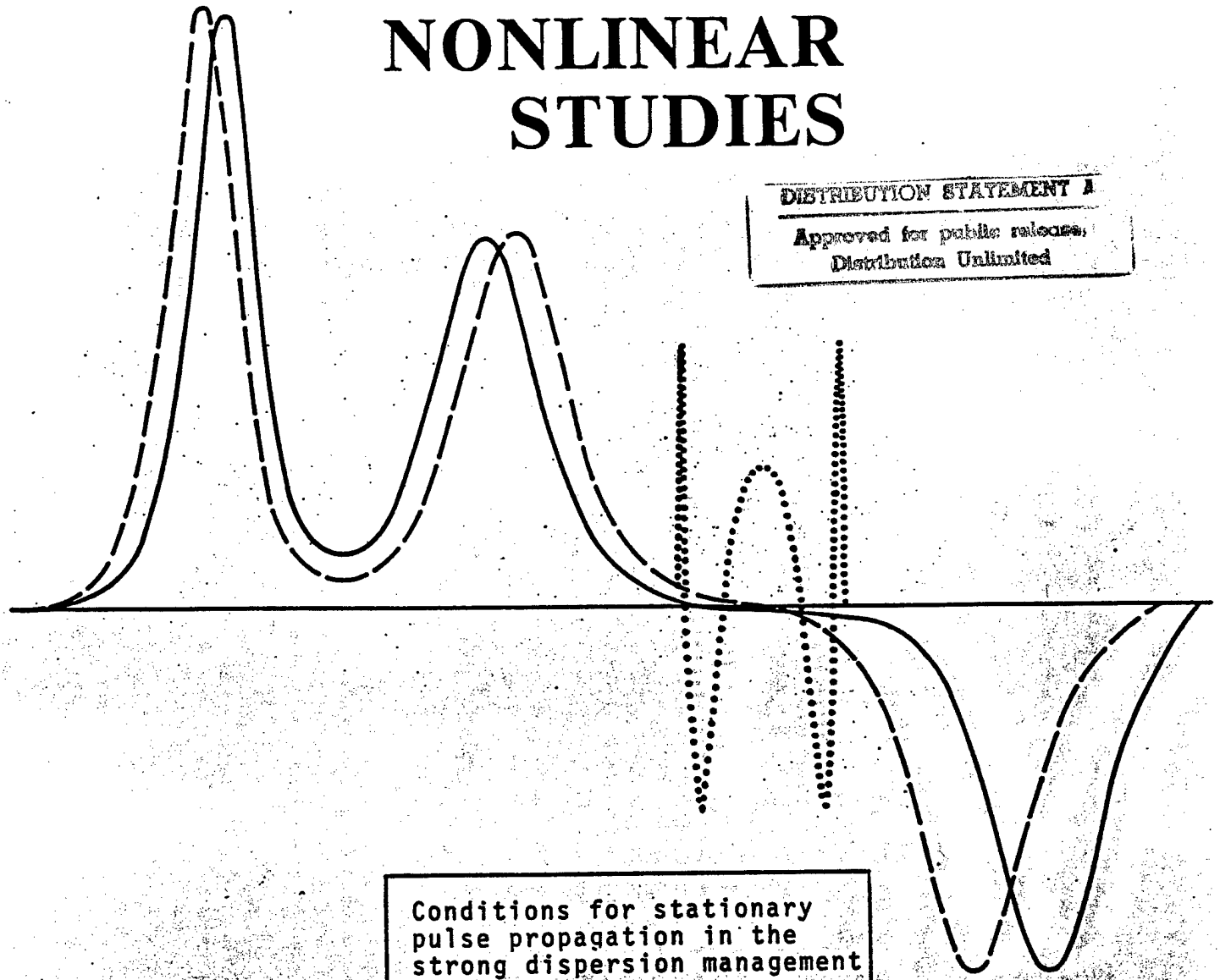

Conditions for stationary pulse propagation in the strong dispersion management regime

BY:
T.I. Lakoba
J.Yang
D.J. Kaup
and
B.A. Malomed

October 31, 1997

CLARKSON UNIVERSITY
Potsdam, New York 13699-5815, U.S.A.

19980423 010

DTIC QUALITY INSPECTED 3

Conditions for stationary pulse propagation in the strong dispersion management regime

T.I.Lakoba*
Department of Mathematics and Computer Science
Clarkson University, Potsdam, NY 13699-5817, USA

J.Yang
Department of Mathematics and Statistics
The University of Vermont, Burlington, VT 05401

D.J.Kaup
Department of Mathematics and Computer Science
and Department of Physics
Clarkson University, Potsdam, NY 13699-5815, USA

B.A.Malomed
Department of Interdisciplinary Studies, Faculty of Engineering
Tel Aviv University, Tel Aviv 69978, Israel
E-mail: malomed@eng.tau.ac.il

October 31, 1997

Abstract

Using the variational method, we obtain analytical conditions for stationary propagation of a Gaussian pulse in a fibre with strong dispersion management. We consider both the lossless fibre and the one with losses and periodic amplification. The analytical predictions have been checked against direct numerical simulations, and a good agreement between the two has been demonstrated. In particular, we find that in a certain region of parameters, the average dispersion necessary to support the stationary propagation is negative (normal). We also show that under a certain assumption, the variance of the Gordon–Haus timing jitter for the pulse in a strongly dispersion–managed system approximately equals that for the conventional soliton, reduced by an energy enhancement factor. Using our analytical conditions, we obtain an estimate for this factor. In particular, we show that in the presence of losses and periodic amplification, this jitter suppression factor can be made to be as large as that for the lossless case, by properly choosing the segment lengths in the dispersion map.

*Corresponding author. E-mail: lakobati@sun.mcs.clarkson.edu

PACS: 42.65.T, 03.40.Kf

Key words: dispersion management, dispersion compensation, optical solitons, variational method, jitter suppression.

1 Introduction

The technique of dispersion compensation, or dispersion management (DM), for pulse propagation in telecommunication lines has been a subject of intensive theoretical and experimental research in the last few years (see [1]–[18] and references therein). We will be using the acronym "DM" for both "dispersion management" and "dispersion managed", since this will not result in a confusion. For the sake of brevity, we will call the pulse in a DM line a "DM soliton". The DM technique uses periodically concatenated pieces of fibre with opposite signs of dispersion. One advantage of the DM technique over conventional soliton propagation in a uniform fibre is that it allows one to reduce the four–wave mixing, which occurs due to the fibre nonlinearity. The four–wave mixing has been shown [19] to be detrimental for wavelength-division multiplexing (WDM) in a conventional soliton transmission line. Another advantage of the DM technique is that it allows one to keep the average dispersion small, which reduces the Gordon–Haus (GH) timing jitter [20]. Moreover, it has been recently suggested on the basis of a numerical evidence [2, 17] and experimentally verified [3] that the GH jitter in a DM line is reduced compared to that jitter in a uniform fibre with the same average dispersion. In Ref. [3], it was concluded that the corresponding jitter suppression factor is approximately equal to the energy enhancement factor, i.e. the ratio of the pulse energy in the DM line to that of the pulse with the same width in the uniform fibre [2, 3, 4]. Another nontrivial feature of the jitter suppression by means of DM was revealed in Ref. [17], where a model that took into account losses and periodic amplification was studied numerically. The results of [17] showed a strong dependence of the jitter suppression upon the DM period. In Ref. [18], it was further shown that in a modified model where the average dispersion $D_0 \sim 1/z$, i.e. slowly decreases with the propagation distance z, the mean squared jitter grows proportionally only to z, rather than to z^3, as occurs in the GH theory for the nonlinear Schrödinger (NLS) soliton.

Although several attempts at developing a systematic theory of the DM soliton have been made [21, 4, 5, 6], such a theory is still far from being complete. The regime of the so–called weak DM, when the local dispersion lengths are of the order of magnitude of the nonlinear length, has been studied in most detail [22, 21, 4, 5]. It is the strong DM regime, when the local dispersion lengths are much smaller than the nonlinear length, that is both the most interesting for the applications and also the most difficult for the analysis (we note that this regime has been recently analyzed in [6] using the Lie transformation). However, in the strong DM regime, the following simplification occurs: Since the local dispersion, but not the nonlinearity, is the main factor affecting the pulse propagation, then that pulse must resemble some particular exact solution of the linear part of the evolution. Numerical findings of [7, 8, 9], and of a number of other studies, indicate that this particular solution must be a Gaussian pulse.

In this work, we employ the variational method to obtain the conditions for the stationary propagation of a pulse in the strong DM regime. We consider both the case of a lossless fibre and the case where losses and periodic amplification are present in the transmission line. It should be noted that the variational method has been previously used [10, 11, 12, 13, 14] to study the DM soliton, with the last two papers specifically focusing on determining the stationary propagation conditions. One of the

two conditions (the one related to the initial chirp of the pulse) that we obtain here is the same as was obtained in [13, 14] and in a number of numerical studies. The other condition, which relates the average dispersion to the pulse's maximum amplitude, appears to be different. In particular, we find that this latter condition predicts, quite unexpectedly, that a DM soliton can propagate stationarily when the average dispersion is *negative* (i.e. normal). To verify the conditions obtained, we ran a series of extensive numerical simulations. The numerical results were found to agree quite well with our analytical predictions.

In the second part of our work, we follow the standard procedure ([20], see also Sec.8.1 in [23]) and derive the GH timing jitter for the DM soliton. We point out that such a derivation requires a certain assumption about the orthogonality of the solutions of the linearized evolution equation in question. With that assumption, we can recover the standard GH result, and then can estimate the jitter suppression factor as a function of the dispersion map parameters. In particular, we show that by properly choosing the segment lengths in the dispersion map, one can make the jitter suppression factor in a system with losses and periodic amplification to be almost as large as that in the corresponding lossless system.

2 Variational approximation

Pulse propagation in a DM transmission line is conventionally described by the following equation:

$$iU_Z + \frac{1}{2}\tilde{D}(Z)U_{TT} + \tilde{G}(Z)U|U|^2 = 0\,, \tag{1}$$

where Z, T, and U are the coordinates and the electric field amplitude, $\tilde{D}(Z)$ is the local dispersion coefficient, and $\tilde{G}(Z)$, whose form will be specified later, accounts for the damping and periodic amplification of the pulse (see, e.g., [23]). Note that in Eq. (1), $\tilde{D} = -\partial^2 k/\partial\omega^2$ (where k and ω are, respectively, the wave vector and frequency of the carrier); thus the units of $\tilde{D}$ are [s^2/m]. The form of the periodic function $\tilde{D}(Z)$ (of period $L_{\rm map}$) is

$$\tilde{D}(Z) = \begin{cases} \tilde{D}_1\,, & 0 < \mathrm{mod}(Z,\, L_{\rm map}) < \tilde{L}_1\,, \\ \tilde{D}_2\,, & \tilde{L}_1 < \mathrm{mod}(Z,\, L_{\rm map}) < L_{\rm map}\,, \end{cases} \tag{2}$$

with $\tilde{D}_1\tilde{D}_2 < 0$. The strong DM regime corresponds to the situation where $L_{\rm map} \ll 1/(\tilde{G}|U_0|^2)$ and $|\tilde{D}_1\tilde{L}_1| \approx |\tilde{D}_2\tilde{L}_2| \sim \tau_p^2$. Here $|U_0|^2$ is the pulse peak power, τ_p is the pulse width, and $\tilde{L}_2 = L_{\rm map} - \tilde{L}_1$. If we introduce new, nondimensional variables: $z = Z/L_{\rm map}$, $\tau = T/\sqrt{\tilde{L}_1\tilde{L}_2|\tilde{D}_1 - \tilde{D}_2|/L_{\rm map}}$, and $u = U/U_0$, then Eq. (1) takes on the form:

$$iu_z + \frac{1}{2}D(z)u_{\tau\tau} + \epsilon\left[\frac{1}{2}D_0 u_{\tau\tau} + G(z)u|u|^2\right] = 0\,. \tag{3}$$

Here $\epsilon = L_{\rm map}|U_0|^2$ and

$$D(z) = \begin{cases} D_1 = \dfrac{\mathrm{sgn}(\tilde{D}_1 - \tilde{D}_2)}{L_1}\,, & 0 < \mathrm{mod}(z\,,1) < L_1\,, \\ D_2 = \dfrac{\mathrm{sgn}(\tilde{D}_2 - \tilde{D}_1)}{L_2}\,, & L_1 < \mathrm{mod}(z\,,1) < 1\,, \end{cases} \tag{4}$$

$L_{1,2} = \tilde{L}_{1,2}/L_{\rm map}$, $D_0 = (\tilde{D}_1\tilde{L}_1 + \tilde{D}_2\tilde{L}_2)/(\tilde{L}_1\tilde{L}_2|\tilde{D}_1 - \tilde{D}_2|\,|U_0|^2)$, and $G(z) = \tilde{G}(Z/L_{\rm map})$. Note that for the variables scaled as in Eq. (3), one has the dispersion map period unity and

$$D_1L_1 + D_2L_2 = 0, \qquad |D_1L_1| = |D_2L_2| = 1\,. \tag{5}$$

The following important remark regarding the meaning of the small parameter ϵ in Eq. (3) is in order here. In the discussion in Section 3 below, we will consider the maximum amplitude A of the soliton to be of order unity. Then ϵ is on the order of magnitude of the ratio of the local dispersion length to the nonlinear length in the system. On the other hand, as we will show below, the average dispersion D_0 that will be necessary for stationary propagation of a pulse can be rather small. Thus, if one defines the measure of the "strength" of the DM in a given fibre to be the ratio of the average and local dispersion lengths (as it was implied in the majority of numerical and experimental studies), then that "strength" parameter, $1/(\epsilon D_0)$, can actually be much greater than $1/\epsilon$.

A well known particular solution of Eq. (3) with $\epsilon = 0$ is the Gaussian pulse

$$u_0 = \frac{A}{\sqrt{1 + 2i(\Delta/\tau_0^2)}} \exp\left[-\frac{\tau^2}{(\tau_0^2 + 2i\Delta)} + i\phi\right]. \tag{6}$$

Here A and τ_0 are, respectively, the maximum amplitude and minimum width of the pulse over one map period, $\Delta(z) = \Delta_0 + \int_0^z D(z')dz'$, and Δ_0 and ϕ are real constants. In the majority of previous studies, the same ansatz has been used, but in a different form:

$$u_0 = a(z) \exp\left[-\frac{\tau^2}{W^2(z)} + ic(z)\tau^2 + i\phi\right]. \tag{6'}$$

The relation between the so introduced quantities: complex amplitude $a(z)$, width $W(z)$, and chirp parameter $c(z)$, on one hand, and the parameters used in Eq. (6), on the other, is as follows:

$$a(z) = \frac{A}{\sqrt{1 + 2i(\Delta/\tau_0^2)}}, \qquad W(z) = \frac{\sqrt{\tau_0^4 + 4\Delta^2}}{\tau_0}, \qquad c(z) = \frac{2\Delta}{\tau_0^4 + 4\Delta^2}. \tag{7}$$

Our goal is to determine for what values of these parameters the pulse, whose form is assumed to be close to (6), will propagate stationarily when ϵ in Eq. (3) is small but nonzero. Following [24], we insert the ansatz (6), in which A, τ_0, Δ_0, and ϕ are now allowed to change slowly with z, into the Lagrangian density of Eq. (3) and integrate over τ. The resulting reduced Lagrangian is then used to obtain the evolutions of these four parameters. The phase ϕ is eliminated by simple algebra, and then one obtains the following three equations:

$$A^2\tau_0 \equiv E = \text{const}, \tag{8a}$$

$$\frac{d\tau_0}{dz} = \sqrt{2}\,\frac{\epsilon G(z) E \tau_0 \Delta(z)}{W^3(z)}, \tag{8b}$$

$$\frac{d\Delta_0}{dz} = \epsilon D_0 + \frac{\epsilon G(z) E\,[4\Delta^2(z) - \tau_0^4]}{2\sqrt{2}\,W^3(z)}. \tag{8c}$$

Note that for the specific form of ansatz (6), the perturbation terms in Eq. (3) are even functions of τ. Thus they will not change the soliton's velocity and centre coordinate, and therefore we need not include the latter two parameters in the variational ansatz.

The conditions for the stationary propagation of a pulse require that its amplitude and width remain, on average, the same when z is increasing [13, 14]. This is so if $\tau_0(z) = \tau_0(z+1)$ and $\Delta_0(z) = \Delta_0(z+1)$ (recall that $L_{\text{map}} = 1$ in the units of Eq. (3)). Moreover, from Eqs. (8) one sees that τ_0 and Δ_0 can change by no more than $O(\epsilon)$ within one map period. Thus, it is legitimate to obtain the first–order

conditions in question, by inserting into (8b) and (8c) the unperturbed values for τ_0 and Δ_0, and requiring that

$$\int_0^1 \frac{d\tau_0}{dz}\,dz = \int_0^1 \frac{d\Delta_0}{dz}\,dz = 0\,. \tag{9}$$

Then these two conditions become, respectively:

$$\int_{-1/2}^{1/2} \frac{[s+\Delta_0+\frac{1}{2}]\,g(s)ds}{\left[\tau_0^4+4(s+\Delta_0+\frac{1}{2})^2\right]^{3/2}} = 0\,, \tag{10a}$$

$$D_0 = -\frac{\sqrt{2}}{4}A^2\tau_0^4\int_{-1/2}^{1/2} \frac{[4(s+\Delta_0+\frac{1}{2})^2-\tau_0^4]\,g(s)ds}{\left[\tau_0^4+4(s+\Delta_0+\frac{1}{2})^2\right]^{3/2}}\,, \tag{10b}$$

where

$$g(s) = L_1 G\left(L_1(s+\frac{1}{2})\right) + L_2 G\left(L_1+L_2(\frac{1}{2}-s)\right)\,. \tag{11}$$

Eqs. (10) and (11) can be obtained from Eq. (9) in the following way. First, one integrates over z from 0 to L_1 and makes the variable substitution $z = L_1(s+1/2)$. Then one adds to this result, the integral over $L_1 < z < 1$, in which one needs to make the variable substitution $(z-L_1) = L_2(1/2-s)$. Then with (5), one obtains Eqs. (10) and (11).

Conditions (10) have the following meaning. The first condition determines Δ_0 and hence the initial chirp (cf. Eq. (7)) which results in the pulse propagating stationarily down the DM fibre. Then the second condition determines the maximum amplitude required for the stationary propagation for a given average dispersion of the system.

3 Comparison of analytical conditions (10) with numerical results

We now consider different configurations of the periodic amplification relative to the periodic dispersion map. The simplest case is when one has no losses and amplification, so that $G(z) \equiv 1$, and then $g(s) \equiv 1$. In this case, the integrals in Eqs. (10) can be evaluated explicitly, yielding:

$$\Delta_0 = -\frac{1}{2}\,, \tag{12a}$$

$$D_0 = -\frac{\sqrt{2}}{4}A^2\tau_0^4\left[\ln\left(\sqrt{1+\frac{1}{\tau_0^4}}+\frac{1}{\tau_0^2}\right) - \frac{2}{\sqrt{\tau_0^4+1}}\right]\,. \tag{12b}$$

Conditions (8a) and (12a), expressed in a different but equivalent form, have been previously obtained analytically in [13, 14]. Condition (12a) has also been found numerically in, e.g., [15, 9, 8]. This condition requires that the pulse have zero chirp at midpoint of each fibre segment. Condition (12b) coincides with the condition obtained in [14] when $\tau_0^2 \gg 1$, which is where the approximation made in that paper is only expected to work well; cf. Fig. 2 in [14]. (Since in Eq. (12b) and in subsequent formulae, it is τ_0^2 and its powers, rather than τ_0 itself, that appear, then we will refer to the parameter τ_0^2 in our discussion below.) Eq. (12b) is also different from the corresponding condition derived earlier in Ref. [13]. (The approaches adopted in Ref. [13] and in the present work appear to be technically not equivalent; however, a detailed comparison of these approaches and their results is outside the scope of this paper.) Note that Eq. (12b) also predicts, quite unexpectedly, that the DM soliton can propagate stationarily for *negative* D_0 provided that $\tau_0^2 < (\tau_0^2)_{\rm th} \approx 0.30$. To our knowledge, this fact has never been reported before. (Note that the expression derived in Ref. [13] did not predict the sign of D_0, but only its absolute value.)

In order to verify the validity of Eqs. (10) (and, in particular, of Eqs. (12) for the lossless case), we solved Eq. (3) numerically, with the parameters of the initial Gaussian pulse (6) being taken as predicted by these equations. We used the pseudo–spectral method in τ and the fourth–order Runge–Kutta method in z. The value of ϵ in all our simulations was set to 0.1. For the lossless case, we also fixed $L_1 = 0.4$, $L_2 = 0.6$, $D_1 = 1/L_1$ and $D_2 = -1/L_2$, and then the only free parameter of a pulse with a unit maximum amplitude (i.e. with $A = 1$) was its minimum width, τ_0. The average dispersion, D_0, in Eq. (3) was set in accordance with Eq. (12b). The simulations were run for a number of values of the parameter τ_0^2 in the range from 0.05 to 3.0; cf. Fig. 1. In each run, we measured the value of τ_0 when the pulse appeared to reach a (quasi–) stationary regime. Then for each τ_0 so obtained, we plotted, in Fig. 1, the ratio of the average dispersion to the pulse energy, along with the corresponding analytical curve. The agreement between the theory and the numerics is seen to be good.

In Fig. 2, we showed the pulse evolution for two typical cases where τ_0^2 is initially 0.2 and 0.5. For all τ_0^2 greater than the threshold value, $(\tau_0^2)_{\rm th}$, the maximum and minimum amplitudes of the pulse do not settle down to constant values, but instead undergo almost periodic, long–term and small–amplitude oscillations (Fig. 2a). In this case, very small continuum radiation from the pulse is seen in the numerics. On the other hand, for $\tau_0^2 < (\tau_0^2)_{\rm th}$, the pulse amplitudes undergo a very slow decay, occurring with an approximately constant rate, due to emission of continuum radiation. The amount of this radiation is still quite small, so that the amplitudes of the pulse with the initial value of $\tau_0^2 = 0.2$ decrease by less than 10% over the distance $z = 800$ (Fig. 2a). Even though this decay intensifies for pulses with smaller initial values of τ_0^2, we still observed that even for τ_0^2 as small as 0.05, the amplitudes of the pulse decay only by about 10% over a distance as large as $z = 600$. (However, rigorously speaking, there exist no (quasi–) stationary pulses for $\tau_0^2 < (\tau_0^2)_{\rm th}$. Thus we did not plot the corresponding numerical results in Fig. 1.) It is also worth noting that despite the fact that, for large z, the amplitude evolution within one period of the dispersion map becomes noticeably different from that assumed by ansatz (6) (cf. Fig. 2b), the stationarity conditions (10) (and, in particular, (12)), which were derived using that ansatz, still continue to hold remarkably well.

We also note that for relatively large values of τ_0^2 ($\tau_0^2 > 2.0$), the long-term oscillations of the pulse amplitudes look more like those of an NLS soliton launched with a slightly "wrong" initial amplitude (see, e.g., [25]). In fact, this is to be expected: for larger pulse widths, the magnitude of the second term in Eq. (3) decreases compared to the magnitude of the last term (recall that the maximum pulse amplitude is unity). Thus for large τ_0, the nonlinear term plays a larger role in the evolution than it does for small τ_0, and therefore the equation becomes closer to the NLS equation. This is also consistent with the asymptotics of Eq. (12b) for large τ_0^2, where one finds that the product $A\tau_0$ is proportional to $D_0^{1/2}$, which is characteristic of an NLS soliton. (This was also pointed out earlier in Ref. [13].)

When there are losses and periodic amplification in the transmission line, then possible configurations of the periodic dispersion map relative to the amplification pattern become numerous. Here we will only consider three of them, which are representative of those cases that seem to be the most interesting from the viewpoint of applications. First, we consider the situation when the amplification and the dispersion map periods coincide, so that $L_{\rm amp} = 1 (= L_{\rm map})$ and $G(z) = \exp(-2\alpha \,{\rm mod}(z\,,1))$. Here α is the damping coefficient. In such a case, $g(s)$ in Eq. (11) takes on the form:

$$g(s) = e^{-\alpha L_1}\left[L_1 e^{-2\alpha L_1 s} + L_2 e^{-\alpha + 2\alpha L_2 s}\right]. \tag{13}$$

Since $L_1 + L_2 = 1$, then the integrals in (10) depend on three parameters: τ_0, α, and, say, L_1. We took $\alpha = 1.013$ (which in physical units corresponds to $2\alpha = 0.22\,{\rm dB/km}$ and $L_{\rm amp} = 40\,{\rm km}$) and numerically calculated Δ_0 and the ratio (D_0/E) from Eqs. (10) as functions of τ_0 for several different

values of L_1, in the range from 1/6 to 5/6. We note that in both these and the previous (i.e. lossless) cases, a unique value of Δ_0 was found for each τ_0.

Our results for $\Delta_0(\tau_0)$ are plotted in Fig. 3a. Next, for all values of L_1, the curves showing the dependence of (D_0/E) on τ_0 are very close to each other for all τ_0^2 that are just slightly larger than the threshold value $(\tau_0^2)_{\rm th}$. Therefore, in Fig. 1 we only plotted one theoretical curve in this case, corresponding to $L_1 = 7/18$ (dashed line). The reason for choosing this particular L_1 will be explained later. The results of numerical simulations of Eq. (3) for $L_1 = 7/18$ are plotted with squares. Also in the same figure, we plotted the results of numerical simulations for $L_1 = 2/3$ (triangles). The agreement between the theory and the numerics is again seen to be good. The long–term oscillations of the pulse's maximum and minimum amplitudes were found in this case to have significantly larger periods (by more than a factor of two) than it was, for the same initial values of τ_0^2, in the lossless case (cf. Fig.2a).

Next, we considered two cases with: (i) $L_1 = 4L_{\rm amp}$, $L_2 < L_{\rm amp}$, and (ii) $L_2 = 4L_{\rm amp}$, $L_1 < L_{\rm amp}$. Cases (i) and (ii) correspond to the situations when the dispersion accumulated over four consecutive amplification periods in the fibre is compensated by a short piece of fibre with the opposite sign of dispersion just before and just after an amplifier, respectively. These cases are sometimes referred to in the literature as a postcompensation and a precompensation schemes, respectively (see, e.g., [11]). The proportionality coefficient of 4 between the longer segment of the map and $L_{\rm amp}$ was taken somewhat arbitrarily, although it does correspond to the experimental setups considered in [16, 3]. These cases are also close to the one for which the jitter suppression factor was found to be maximum in Ref. [17]. In case (i), $G(z) = \exp\left[-2\alpha\left(\frac{z}{L_{\rm amp}} - k\right)\right]$ for $kL_{\rm amp} \le z < (k+1)L_{\rm amp}$ $(k = 0, 1, 2)$ and for $3L_{\rm amp} \le z < 1$ $(k = 3)$. In case (ii), $G(z) = \exp\left[-2\alpha\left(\frac{z-L_1}{L_{\rm amp}} - k\right)\right]$ for $0 \le z < L_{\rm amp} + L_1$ $(k = 0)$ and for $kL_{\rm amp} \le (z - L_1) < (k+1)L_{\rm amp}$ $(k = 1, 2, 3)$. The corresponding forms of $g(s)$ can easily be found to be as follows:

$$\text{case (i)} \qquad g(s) = L_1\tilde{g}(s) + L_2 \exp\left[-\alpha\left(2 + \frac{L_2}{L_{\rm amp}}(1-2s)\right)\right], \tag{14a}$$

$$\text{case (ii)} \qquad g(s) = L_1 \exp\left[\alpha\frac{L_1}{L_{\rm amp}}(1-2s)\right] + L_2\tilde{g}(-s), \tag{14b}$$

where $\tilde{g}(s) = \exp\left[-8\alpha\left(s - \frac{k}{4}\right)\right]$ for $\frac{k}{4} \le s < \frac{k+1}{4}$ $(k = -2, -1, 0, 1)$.

The value of the damping parameter, $(\alpha L_{\rm map})$, in cases (i) and (ii) was taken to be the same as in the case with $L_{\rm map} = L_{\rm amp}$, i.e. $\alpha L_{\rm map} = 1.013$. In compliance with the numerical observations of Ref. [15] (although made for a slightly different configuration), we found that Eqs. (10), with $g(s)$ given by Eqs. (14), yield solutions that are only slightly different from those in the lossless case (see Eqs. (12)). In case (i), the curves $\Delta_0(\tau_0)$ for all values of $L_2/L_{\rm amp}$ from 0.1 to 0.5 are essentially indistinguishable in the plot. Thus we only plotted one such curve, for $L_2/L_{\rm amp} = 0.1$ (Fig. 3b). In case (ii), $\Delta_0(\tau_0)$ depends slightly on the ratio $L_1/L_{\rm amp}$, with $\Delta_0(\tau_0)$ increasing monotonically with $L_1/L_{\rm amp}$ for all τ_0 (cf. Fig. 3b). The values of (D_0/E) in case (i), as well as these values for $L_1/L_{\rm amp} = 0.1$ in case (ii), are very close to those values found in the case $L_{\rm map} = L_{\rm amp}$; therefore we did not plot them in Fig. 1. We plotted only the corresponding curve for case (ii) with $L_1/L_{\rm amp} = 0.5$ (dash–dotted line), which is the most distinct from the other two curves in Fig. 1. Since the numerical simulations confirmed the validity of our analytical predictions in the previous cases, we did not perform simulations for cases (i) and (ii).

The proximity of the results obtained in cases (i) and (ii) to those obtained in the lossless case holds, however, only for $\tau_0^2 > (\tau_0^2)_{\rm th}$. (This threshold differs slightly from case to case and from one value of $L_1/L_{\rm amp}$ or $L_2/L_{\rm amp}$ to another within the same case, but it remains close to its value in the

lossless case, $(\tau_0^2)_{\rm th} \approx 0.30$.) For $\tau_0^2 < (\tau_0^2)_{\rm th}$, there exist more than one (up to seven, for very small τ_0) values of Δ_0. As an example, we considered case (i) with $L_2/L_{\rm amp} = \tau_0^2 = 0.15$, where there exist five values of Δ_0. These values were computed numerically from Eq. (10a). Three of them are less than -0.5 and the other two are greater than -0.5. All five of the corresponding values of the average dispersion, given by Eq. (10b), are negative, and their magnitudes can vary by more than a factor of three depending on what particular Δ_0 is taken. We performed simulations for the maximum amplitude A being initially unity in all those cases, and the initial pulse chirp and the average dispersion in the system taken according to Eqs. (10). The pulse evolution was followed up to $z = 300$. In all these five cases, we observed that the evolution was essentially similar to that in other cases when the initial parameter τ_0^2 was less than the threshold value and the average dispersion was negative. In particular, we observed a buildup of a small amount of radiation near the core of the pulse as well as a slow and monotonic change of the pulse's maximum amplitude.

Finally, we also numerically investigated the stability of a DM soliton against relatively large perturbations of its initial conditions. We restricted our attention to the lossless case, since in the other cases the results are expected to be similar. We ran several simulations where the initial energy of a DM soliton was taken to be by up to 60% different (both greater and less) from the value predicted by Eqs. (8a) and (12b). We considered both cases, of positive and negative average dispersion. In all simulations, we observed that the pulse eventually settles down to a new DM soliton surrounded by continuum radiation (recall that in the case of negative D_0, such a soliton is expected to slowly decay due to its continuous emission of radiation). This behaviour is similar to that of the NLS soliton. However, there are two essential differences from the NLS case, which we will point out. The first one is the observed fact that the radiation remains in the vicinity of a DM soliton for a much longer time (the maximum length of the evolution in this series of our simulations was $z = 800$). The reason is that the variable dispersion $D(z)$ in Eq. (3), that determines the evolution of $u(z,\tau)$ in the leading order, does not allow any initial disturbance to spread out without limit. Indeed, no matter how much the disturbance has spread out during its propagation in one segment of the fibre, this will be precisely undone (when $\epsilon = 0$) in the next segment. Thus it is only the much weaker average dispersion ϵD_0 that forces the radiation to eventually separate from the soliton. The second difference from the NLS case pertains to the evolution of sufficiently narrow ($\tau_0^2 < 0.5$) pulses launched with "wrong" initial conditions. In that case, the parameters of the pulse tend to remain almost unchanged up to a fairly large propagation distance, z_c ($z_c \sim 1/(\epsilon\tau_0^2)$). Then they change, within a much shorter distance, and the modified pulse continues its propagation at new, stationary values of its parameters. This feature of the model is illustrated in Fig. 4.

4 Estimate of the timing jitter suppression for a DM soliton

Having demonstrated that the variational method works well in predicting the initial amplitude and chirp for launching a stationary DM soliton, we will now use the same method to evaluate the GH timing jitter for such a pulse. We will follow the standard derivation for the NLS soliton, but we will need to make a certain assumption in order to obtain the jitter variance for the DM soliton. Proceeding with that assumption will give us the conventional result, and hence allow us to estimate the jitter suppression factor (JSF).

In order to model the (distributed) noise from the amplifiers, we add to the rhs of Eq. (3) a random force $R = R(\tau, z)$, whose variance we assume to be much smaller than ϵ. Then the solution to Eq. (3) is sought in the form: $u = u_0 + u_1 + \ldots$, $|u_1| \ll |u_0|$. Here u_0 is given by Eq. (6) in which the parameters are now slow functions of z, and u_1 is the continuum radiation. Since R *is* expected to affect the pulse

velocity V and centre position τ_c, we need to include these degrees of freedom in the ansatz (6). This can easily be done by using the Galilean and translational invariances of Eq. (3). Following, e.g., [26], one obtains:

$$\int_{-\infty}^{\infty} d\tau \left\{ u_{0,\tau}^{*} \left[\text{lhs of (3)} \right] + c.c. \right\} = \int_{-\infty}^{\infty} d\tau \left\{ \left[u_{0,\tau}^{*} R + c.c. \right] + i\partial_z \left[u_{0,\tau}^{*} u_1 - c.c. \right] \right\} , \tag{15}$$

where the term in square brackets on the lhs of Eq. (15) is evaluated for $u = u_0$ and $c.c.$ stands for the complex conjugate. In [26], where the NLS and other nonlinear evolution equations with constant coefficients were considered, the last term on the rhs of the counterpart of Eq. (15) vanished due to the orthogonality of the radiation field u_1 to the Goldstone mode $u_{0,\tau}$ (see, e.g., [27]). However, this same argument cannot be made at this time for Eq. (3), since the corresponding linearized operator has yet to be studied. Thus nothing is certain about the orthogonality of its eigenmodes. In order to proceed with the above approach, we shall *assume* here that the last term on the rhs of Eq. (15) can be neglected in comparison with the first one. The main reason why we can justify such an assumption is that with it, we will be able to recover the conventional GH result, which was shown to be in good agreement with the experimental results [3]. In fact, in Ref. [3], the values of the GH jitter in a DM line were compared with those values obtained with the Gordon–Haus formula for the NLS soliton with approximately the same width. The agreement between these two sets of data was found to be good when the latter values were reduced by a factor approximately equal to the ratio of the energies of the DM and NLS solitons.

Proceeding with the assumption stated above, we will also obtain that the JSF approximately equals the ratio of those energies, provided that the widths of both pulses are the same. We shall refer to our result as to an *estimate* for the JSF. Such an estimate, although not fully rigorous, is still expected to show the important dependence of the JSF on the parameters of the pulse and the dispersion map. We will then use this estimate to show that: (i) the JSF can be made very large, provided that $\tau_0^2 \approx (\tau_0^2)_{\text{th}}$, and (ii) when losses and periodic amplification are present, the JSF can be very sensitive to the ratio of the lengths of the segments of the dispersion map.

Neglecting the last term on the rhs of Eq. (15) and then proceeding similarly to [20] (see also [23]), one obtains:

$$V_z = \xi(z) , \tag{16}$$

where $\xi(z)$ is the white noise with $\langle \xi(z) \rangle = 0$ and

$$\langle \xi(z) \xi(z') \rangle = \frac{G_a - 1}{2 N_0 L_{\text{amp}}} \frac{\delta(z - z')}{\int_{-\infty}^{\infty} \tau^2 |u_0|^2 d\tau} . \tag{17}$$

Here the angle brackets stand for the average value, G_a is the power gain of the amplifier, and N_0 is the number of photons per unit energy.

The following three remarks about Eqs. (16) and (17) are in order. First, V_z appears in (16) from the term in Eq. (15) with the slow z–derivative: $(u_{0,z})_{\text{slow}} = V_z u_{0,V} + \tau_{c,z} u_{0,\tau_c} + \dots$. Second, in deriving Eqs. (16) and (17) from Eq. (15) in which the last term on the rhs has *already* been dropped, one *again* needs to make an assumption that is equivalent to the one made above. Namely, one needs to assume that the continuum radiation u_1 is orthogonal to the Goldstone mode $u_{0,\tau}$. Indeed, in the derivation of the timing jitter for the NLS, one implicitly used the fact that the perturbation R could be expanded over the complete and orthogonal set of the eigenmodes of the linearized NLS. (A similar point has been recently emphasized in the derivation of the timing jitter for a pulse in a fibre laser [28].) Finally, the third remark is that Gordon and Haus had a slightly different integrand in the denominator of their counterpart of Eq. (17) (for the NLS soliton, they had $(\tanh^2 \tau \text{sech}^2 \tau)$ instead of $(\tau^2 \text{sech}^2 \tau)$

as it would follow from (17)). This, however, does not lead to any significant difference between their result and ours.

From Eq. (17) one easily deduces that the JSF equals:

$$\mathrm{JSF} = \frac{\left(\int_{-\infty}^{\infty} \tau^2 |u_0|^2 d\tau\right)_{\mathrm{DM}}}{\left(\int_{-\infty}^{\infty} \tau^2 |u_0|^2 d\tau\right)_{\mathrm{NLS}}} . \tag{18}$$

Notice that, although this expression is not tantamount to the ratio of the energies of the DM and NLS solitons, its value is expected to be close to that ratio when the widths of the two solitons are the same. The numerator in (18) is evaluated using Eqs. (6) and (10), whereas the denominator is evaluated for the guiding–centre soliton of the NLS that is obtained from Eq. (3) by dropping the term $\frac{1}{2}D(z)u_{\tau\tau}$. The latter soliton has the form (see, e.g., [23]): $(|u_0|^2)_{\mathrm{NLS}} = (a_0 D_0/\tau_0^2)\,\mathrm{sech}^2(\tau/\tau_0)$, where the factor $a_0 = (2\alpha L_{\mathrm{amp}})/(1-\exp(-2\alpha L_{\mathrm{amp}}))$ accounts for the periodic amplification. As it stands in (18), the JSF is z–dependent, because the numerator in (18) is proportional to $W^2(z)$ (see (7)). We then simply average over one map period, obtaining:

$$\mathrm{JSF} \sim -\frac{\tau_0^4 + \frac{1}{3} + (2\Delta_0 + 1)^2}{a_0 \tau_0^6 \, f(\tau_0, L_1, \alpha)} , \tag{19}$$

where $f(\tau_0, L_1, \alpha)$ denotes the integral in Eq. (10b). We remind the reader that our goal here is to obtain the essential dependence of the JSF on the pulse and system parameters. Therefore we are not concerned with the numerical factors of order one that could possibly be introduced by the above averaging and/or by taking the width of the NLS soliton to be the minimum width, τ_0, of the DM soliton, rather than the latter's average width, etc.

Eq. (19) and the previous considerations show that the JSF can be very large near the point where the function $f(\tau_0, L_1, \alpha)$ vanishes (i.e for $\tau_0^2 \approx (\tau_0^2)_{\mathrm{th}}$). Thus, it seems advantageous to launch DM solitons with $\tau_0^2 \approx (\tau_0^2)_{\mathrm{th}}$ in order to achieve a large jitter suppression. On the other hand, near such a point, a so called stretching factor (the ratio of the maximum and minimum widths of the pulse),

$$S \equiv \frac{\sqrt{\tau_0^4 + (1 + |2\Delta_0 + 1|)^2}}{\tau_0^2} , \tag{20}$$

is also rather large. Using pulses with a large stretching factor has the obvious disadvantage that such pulses should be launched at sufficiently large separation in order to prevent their overlapping. Thus, in designing a transmission line for DM solitons, a certain compromise between these two factors must be reached. Another possible technological problem here is that, if one wishes to use pulses with $\tau_0^2 \approx (\tau_0^2)_{\mathrm{th}}$ or less, then the average dispersion has to be made extremely small (cf. Eq. (10b) and also recall that the pulse amplitude cannot be too large, so as not to violate the assumption that the term $\epsilon u|u|^2$ in Eq. (3) is a small perturbation). This might require a very precise tailoring of the parameters of the dispersion map. (On the other hand, as illustrated in Fig. 4, slight fluctuations of the average dispersion may lead to the destruction of a narrow pulse only after a sufficiently large propagation distance.)

In Fig. 5, we plotted the JSF evaluated with Eq. (19) versus the stretching factor (20) for the lossless case and for all the three cases with different periodic amplification patterns considered above. In the case with $L_{\mathrm{map}} = L_{\mathrm{amp}}$ (Fig. 5a), one can see that the JSF significantly depends on the ratio L_1/L_{amp}. The optimal case, where the JSF is even slightly larger than that in the lossless case for the same values of the stretching factor, was found to occur when $L_1/L_{\mathrm{amp}} \approx 7/18$ (for $(\alpha L_{\mathrm{amp}}) = 1.013$). This curve and the one for the lossless case are so close to each other that they are essentially the same curve in the plot. Note that the ordering of the curves in Fig. 5a, for increasing L_1, is: (c), effectively (a), (b),

(d), and then (e). Our prediction of the existence of an optimal ratio $L_1/L_{\rm amp}$ appears to correct the conclusions of paper [9], which predicted the JSF in a DM line *with* losses and periodic amplification to be significantly lower than that in the lossless line. We also note that there appears to be some correlation between the values of Δ_0 and the JSF. First of all, for the optimal ratio $L_1/L_{\rm amp} = 7/18$, $\Delta_0(\tau_0)$ for all but very small τ_0 is very close to its value in the lossless case, i.e. -0.5 (see Fig. 3a). Moreover, for $L_1/L_{\rm amp} = 1/6$ and $L_1/L_{\rm amp} = 2/3$, the curves $\Delta_0(\tau_0)$ are approximately symmetric relative to the line $\Delta_0 = -0.5$ (see Fig. 3a), and the corresponding curves in Fig. 5a are also very close to each other.

The results for the JSF in the cases when either L_1 or L_2 equals $4L_{\rm amp}$, are close to the estimate in the lossless case, as expected (Fig. 5b). In case (i), all the curves are almost the same, irrespective of the ratio $L_2/L_{\rm amp}$. In case (ii), the ratio $L_1/L_{\rm amp} \approx 0.3$ (curve (b)) appears to yield the maximum JSF (for $(\alpha L_{\rm amp}) = 1.013$).

5 Conclusions

In this paper, we have found analytical expressions for the values of the initial chirp and amplitude at which a nearly Gaussian pulse can propagate almost stationarily in the strong DM regime. This was done both for the lossless case and for the case when losses and periodic amplification were present simultaneously. Our analytical results are in good agreement with the numerics. Surprisingly, we also found that a DM soliton can propagate quasi–stationarily in the regime of normal average dispersion, provided that its minimum width is smaller than the threshold value, $(\tau_0^2)_{\rm th}$.

Next, we estimated the GH timing jitter for a DM soliton by assuming that the continuous spectrum of the linearized evolution equation in question would be orthogonal to the bound states. Our justification for making this assumption is that the result obtained in this manner here was earlier shown [3] to be in good agreement with the results of the physical experiment (in [3], the corresponding formula was essentially postulated; cf. also Section 4 above). Having estimated the jitter for a DM soliton and using our analytical conditions of stationary propagation, we then estimated the jitter suppression factor (which shows how much the jitter for a DM soliton is suppressed, compared to the case of its NLS counterpart). We showed that pulses with a relatively large stretching factor (> 2) can have a large JSF. We also demonstrated that by a proper choice of the ratio of the segment lengths in the DM map, the JSF for a system with losses and periodic amplification can be made to be essentially the same as that in the lossless case. In particular, our estimate predicts that a precompensation scheme (case (ii) above) can yield a slightly larger jitter suppression factor than a postcompensation scheme (case (i)).

Acknowledgements

T.I.L. acknowledges a useful discussion with A.N. Pilipetskii and V.S. Grigoryan. B.A.M. appreciates valuable discussions with F. Matera, M. Settembre, A. Mecozzi, D. Frantzeskakis and K. Hizanidis.

T.I.L. and D.J.K. acknowledge partial support from the Office of Naval Research, under Grant No. N00014-95-1-0323, and from the Air Force Office of Scientific Research, under contract number F49620-96-C-0031. J.Y. acknowledges the support of the National Science Foundation under Grant No. DMS-9622802.

References

[1] F.M. Knox, W. Forysiak and N.J. Doran, J. Lightwave Technol. **13** (1995) 1955; N.J. Smith and N.J. Doran, Optics Lett. **21** (1996) 570; M. Nakazawa and H. Kubota, Electron. Lett. **31** (1995) 216; M. Suzuki et al, Electron. Lett. **31** (1995) 2027; S. Wabnitz, Optics Lett. **21** (1996) 638; I. Morita et al, IEEE Photon. Technol. Lett. **8** (1996) 1573; I. Gabitov and S.K. Turitsyn, Optics Lett. **21** (1996) 327.

[2] N.J. Smith, W. Forysiak and N.J. Doran, Electron. Lett. **32** (1996) 2085.

[3] G.M. Carter, J.M. Jacob, C.R. Menyuk, E.A. Golovchenko and A.N. Pilipetskii, Optics Lett. **22** (1997) 513.

[4] T.-S. Yang and W.L. Kath, Optics Lett. **22** (1997) 985.

[5] T. Okamawari, Y. Ueda, A. Maruta, Y. Kodama and A. Hasegawa, Electron. Lett. **33** (1997) 1063.

[6] A. Hasegawa, Y. Kodama and A. Maruta, "Recent progress in dispersion managed soliton transmission technologies", preprint.

[7] N.J. Smith, F.M. Knox, N.J. Doran, K.J. Blow and I. Bennion, Electron. Lett. **32** (1996) 54.

[8] T. Yu, E.A. Golovchenko, A.N. Pilipetski and C.R. Menyuk, Optics Lett. **22** (1997) 793.

[9] M.K. Chin and X.Y. Tang, IEEE Photon. Technol. Lett. **9** (1997) 538.

[10] B.A. Malomed, D.F. Parker and N.F. Smith, Phys. Rev. E **48** (1993) 1418; R. Grimshaw, J. He and B.A. Malomed, Physica Scripta **53** (1996) 385.

[11] A. Berntson, D. Anderson, M. Lisak, M.L. Quiroga-Teixeiro and M. Karlsson, Optics Commun. **130** (1996) 153.

[12] I. Gabitov, E.G. Shapiro and S.K. Turitsyn, Optics Commun. **134** (1997) 317.

[13] B.A. Malomed, Optics Commun. **136** (1997) 313.

[14] M. Matsumoto, Optics Lett. **22** (1997) 1238.

[15] N.J. Smith, N.J. Doran, F.M. Knox and W. Forysiak, Optics Lett. **21** (1996) 1981.

[16] J.M. Jacob, E.A. Golovchenko, A.N. Pilipetskii, G.M. Carter and C.R. Menyuk, IEEE Photon. Technol. Lett. **9** (1997) 130.

[17] B.A. Malomed, F. Matera and M. Settembre, Optics Commun. (1997) to appear.

[18] B.A. Malomed, Optics Commun. (1997) to appear

[19] P.V. Mamyshev and L.F. Mollenauer, Optics Lett. **21** (1996) 396.

[20] J.P. Gordon and H.A. Haus, Optics Lett. **11** (1986) 665.

[21] K.H. Spatschek, S.K. Turitsyn and Yu.S. Kivshar, Phys. Lett. A **204** (1995) 269.

[22] A. Hasegawa and Y. Kodama, Optics Lett. **16** (1991) 1385.

[23] A. Hasegawa, Y. Kodama, *Solitons In Optical Communications* (Clarendon, Oxford, 1995).

[24] D. Anderson, Phys. Rev. A **27** (1983) 3135.

[25] W.L. Kath, N.F. Smyth, Phys. Rev. E **51** (1995) 1484.

[26] A. Bondeson, M. Lisak and D. Anderson, Physica Scripta **20** (1979) 479.

[27] D.J. Kaup, Phys. Rev. A **42** (1990) 5689.

[28] S. Namiki and H. Haus, IEEE J. Quantum Electron. **33** (1997) 649.

Figure Captions

Fig. 1. Comparison of the ratio of the average dispersion to pulse energy, as given by Eq. (10b), with the results of numerical simulations of Eq. (3). Lossless case: solid — theory, circles — numerics. The threshold value $(\tau_0^2)_{\rm th}$ is marked with a tick mark. The following data pertain to the model with losses and amplification. $L_{\rm map} = L_{\rm amp}$, $L_1/L_{\rm amp} = 7/18$: dashed — theory, squares — numerics; $L_{\rm map} = L_{\rm amp}$, $L_1/L_{\rm amp} = 2/3$: triangles — numerics (see main text); $L_{\rm map} = L_1 + 4L_{\rm amp}$, $L_1/L_{\rm amp} = 0.5$: dash-dotted — theory (see main text).

Fig. 2a. Evolution of minimum and maximum pulse amplitudes in the lossless case. Solid — $\tau_0^2 = 0.2$; dashed — $\tau_0^2 = 0.5$. Other parameters are specified in the text.

Fig. 2b. Evolution of the pulse amplitude within one map period in the lossless case; $799 \le z \le 800$. Thick solid — $\tau_0^2 = 0.2$; thick dashed — $\tau_0^2 = 0.5$; thin solid and thin dashed — the corresponding quantities for $0 \le z \le 1$.

Fig. 2c. Pulse profiles for the same parameters as in Fig. 2b. Thick solid — $\tau_0^2 = 0.2$ at $z = 800$; thick dashed — $\tau_0^2 = 0.5$ at $z = 800$; thin solid and thin dashed — the corresponding profiles at $z = 0$. Note that in order to fit both profiles in the same figure, we shifted the centre of the pulse with $\tau_0^2 = 0.2$ from $\tau = 0$ to $\tau = -5$, and the centre of the pulse with $\tau_0^2 = 0.5$ from $\tau = 0$ to $\tau = 10$.

Fig. 3a. $\Delta_0(\tau_0)$ for the case with $L_{\rm map} = L_{\rm amp}$ for the following values of $L_1/L_{\rm amp}$: 5/6 (a); 2/3 (b); 1/2 (c); 7/18 (d); 1/6 (e).

Fig. 3b. $\Delta_0(\tau_0)$ for cases (i) and (ii). (a) — case (i) with any $L_2/L_{\rm amp}$; (b) — case (ii) with $L_1/L_{\rm amp} = 0.5$; (c) — case (ii) with $L_1/L_{\rm amp} = 0.1$. Note that the vertical scale is different from that in Fig. 3a.

Fig. 4. Evolution of a pulse launched with $\tau_0^2 = 0.1$ and $A = 1$ in a line with $D_0 = 0.305$ (this value of D_0 corresponds to $\tau_0^2 = 0.5$ and $A = 1$ in Eq. (12b)). Note that the pulse energy is initially $\sqrt{5}$ less than that of a pulse with $\tau_0^2 = 0.5$ and $A = 1$, which would propagate stationarily at that average dispersion.

Fig. 5a. Jitter suppression factor calculated from Eq. (19). (a) — lossless case (also see main text). Other curves calculated for the case $L_{\rm map} = L_{\rm amp}$ with the following values of $L_1/L_{\rm amp}$: 1/2 (b); 1/6 (c); 2/3 (d); 5/6 (e).

Fig. 5b. Jitter suppression factor calculated from Eq. (19) for cases (i) and (ii). (a) — lossless case (shown for comparison); (b) — case (ii) with $L_1/L_{\rm amp} = 0.3$; (c) — case (i) with any $L_2/L_{\rm amp}$ and case (ii) with $L_1/L_{\rm amp} = 0.1$; (d) — case (ii) with $L_1/L_{\rm amp} = 0.5$.

Fig.1: Ratio of average dispersion to pulse energy

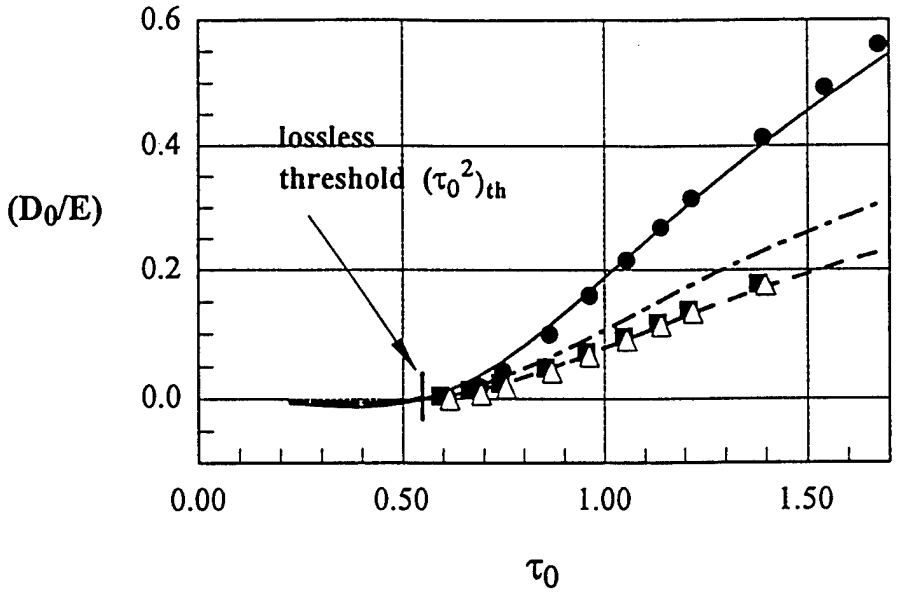

Fig.2a: Evolution of Max and Min amplitudes

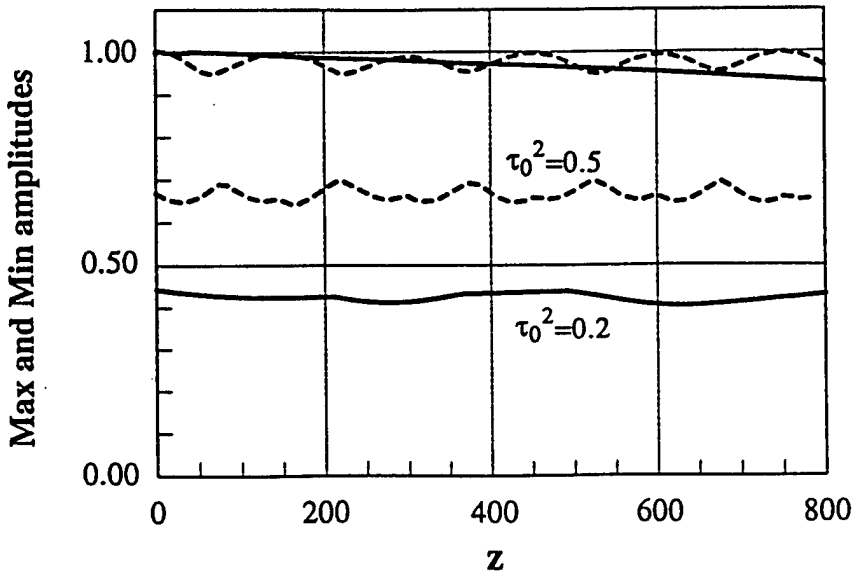

Fig.2b: Evolution of amplitude within one map period

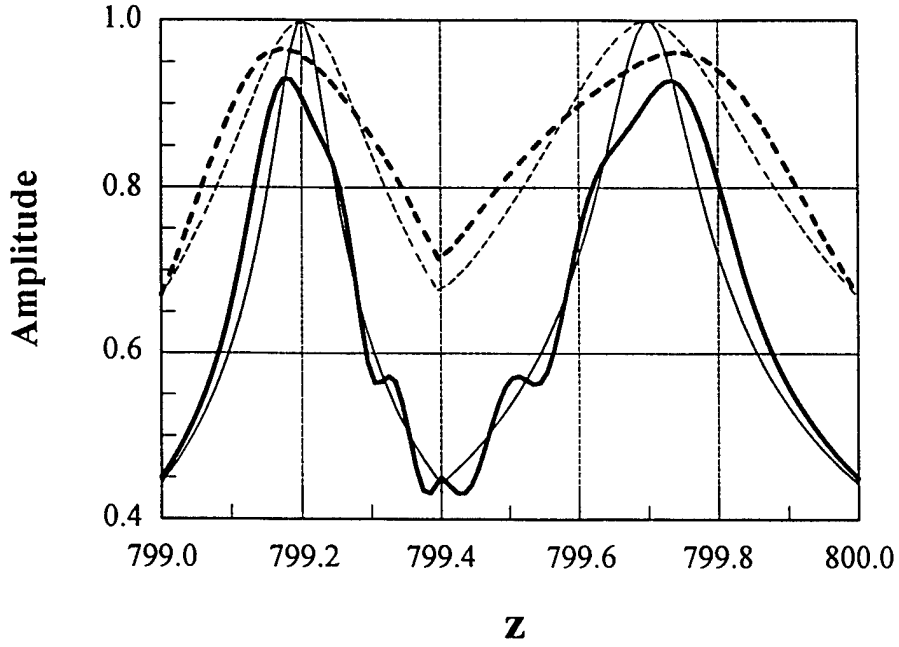

Fig.2c: Comparison of initial and final amplitudes

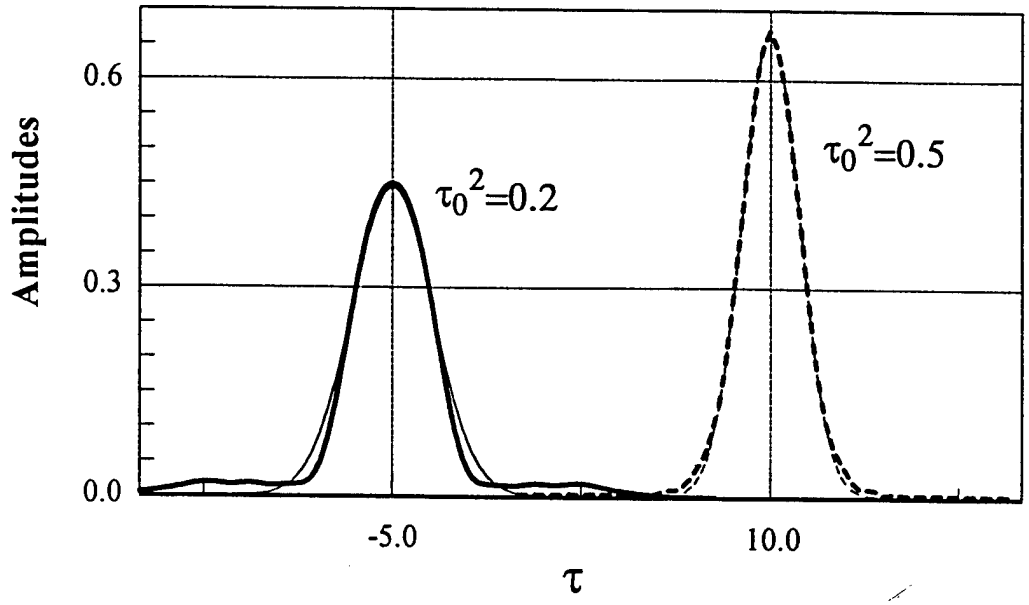

Fig.3a: Δ_0 for the case $L_{map}=L_{amp}$

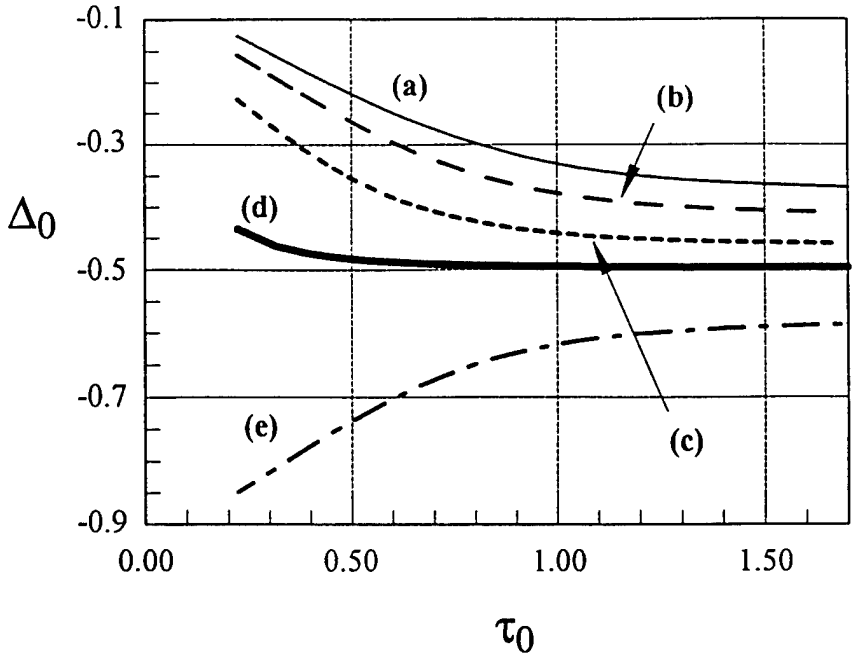

Fig.3b: Δ_0 for cases (i) and (ii)

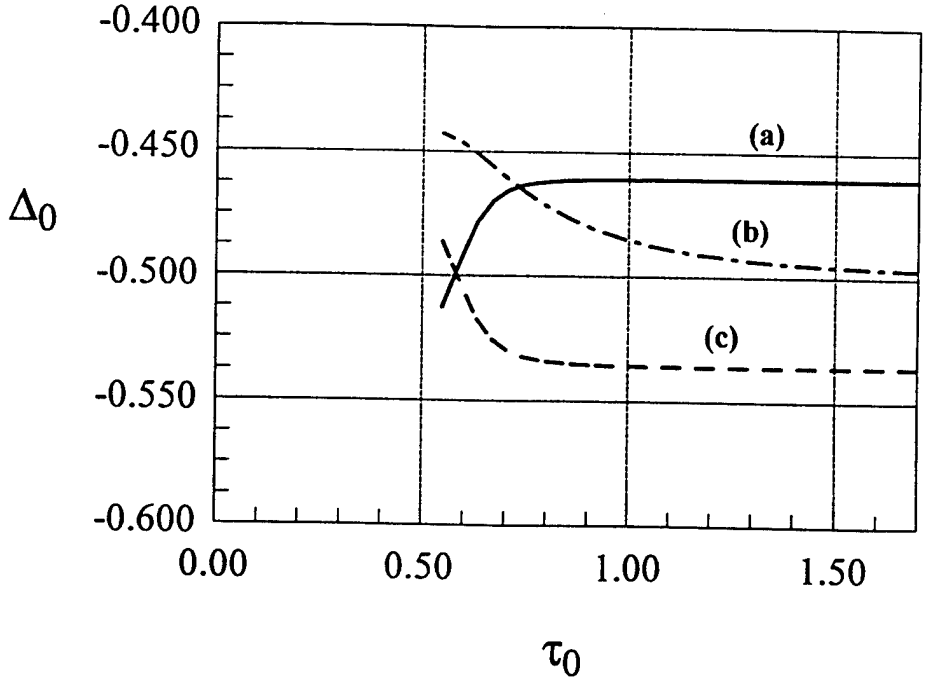

Fig.4: Evolution of a pulse with "wrong" initial parameters

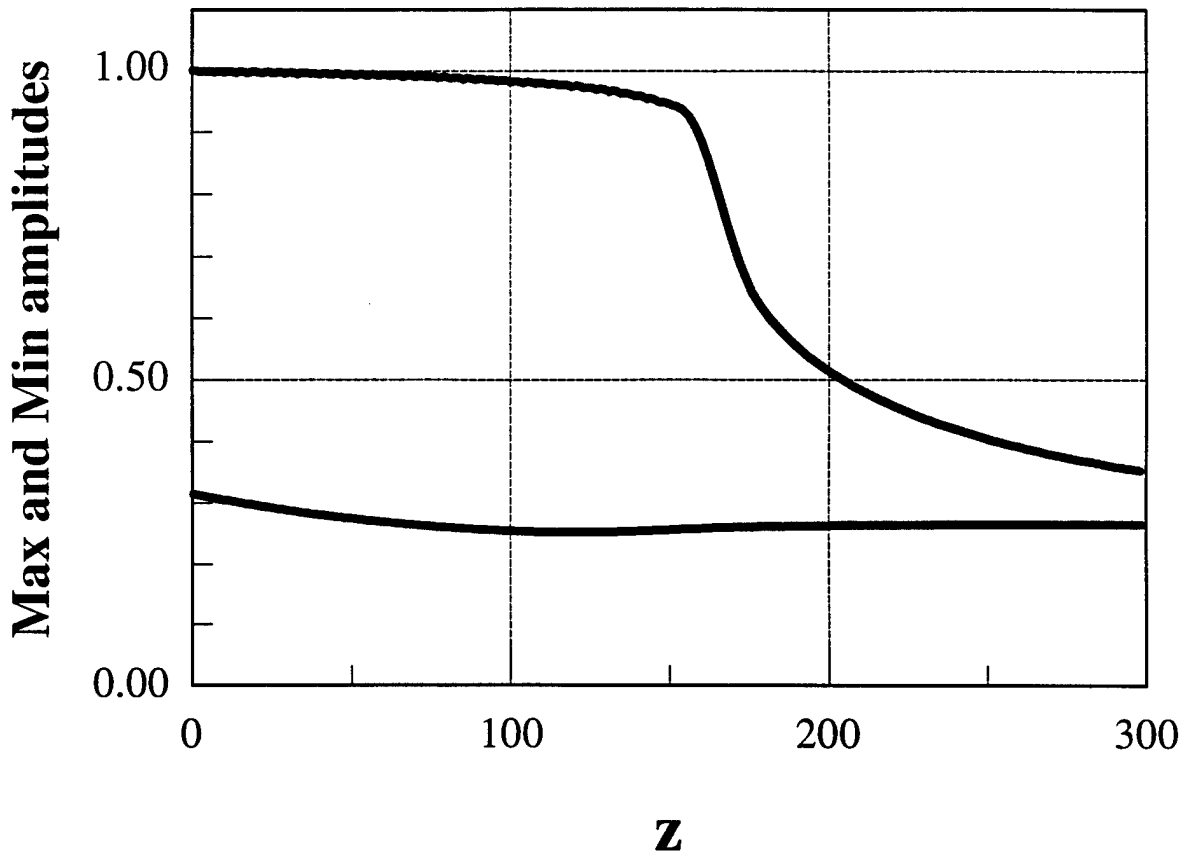

Fig.5a: JSF vs stretching factor (for $L_{map}=L_{amp}$)

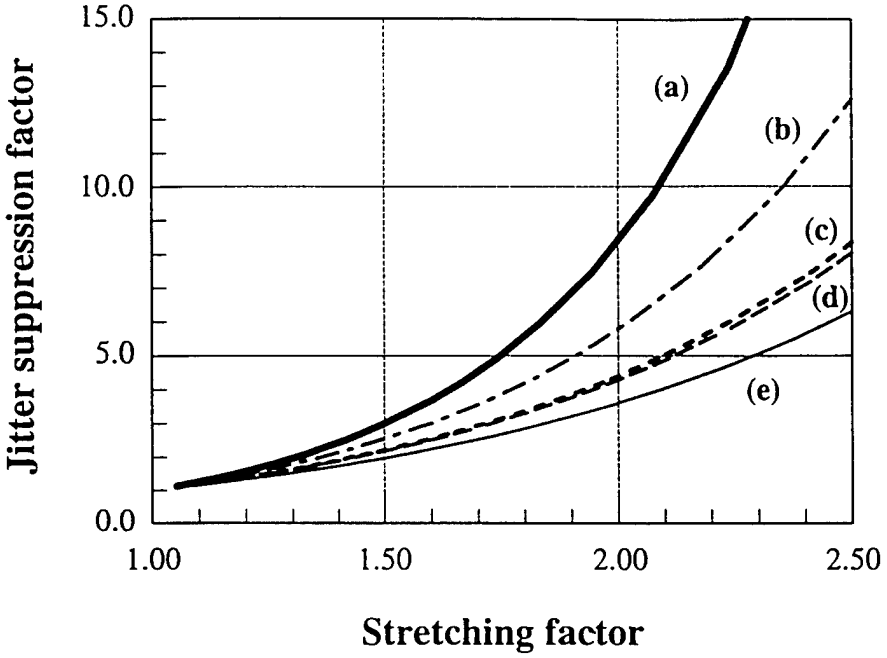
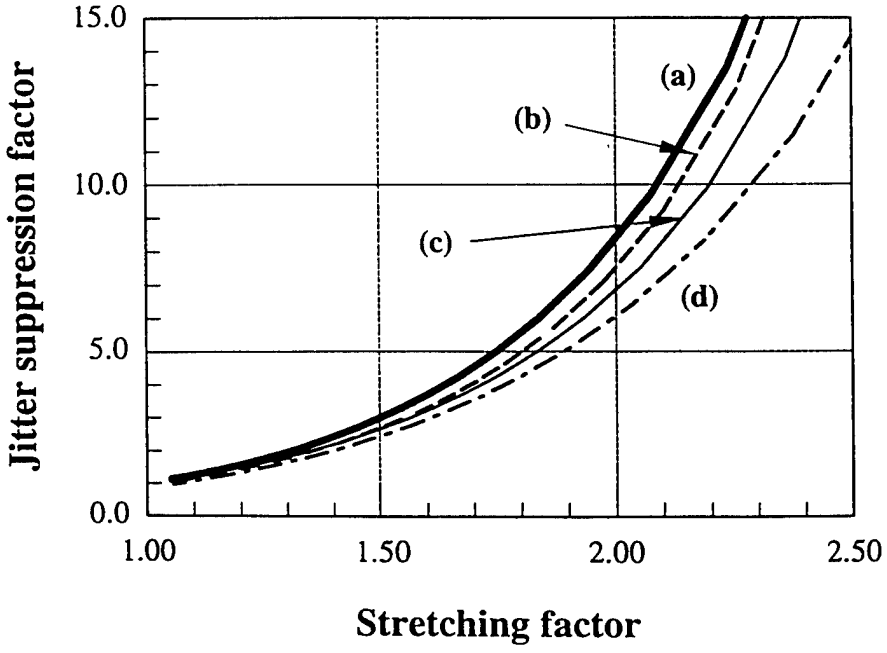
Fig.5b: JSF vs stretching factor
(when either L_1 or L_2 equals $4L_{amp}$)